μTRISTAN

Ryutaro Matsudo

KEK

October 18, 2024

Based on 2201.06664, Yu Hamada (DESY), Ryuichiro Kitano(KEK), RM, Takaura Hiromasa(YITP), Mitsuhiro Yoshida(KEK)
2210.11083, Yu Hamada, Ryuichiro Kitano, RM, Takaura Hiromasa
Work in progress with Lukas Treuer (Sokendai), Shohei Okawa (KEK) Koji Nakamura (KEK), Sayuka Kita (Tsukuba U.) Toshiki Kaji (Waseda U.), Taiki Yoshida (Waseda U.), Kohei Yorita (Waseda U.)

Introduction

- In order to uncover BSM physics, we need to probe higher energy. Higher energy is beneficial not only for direct searches of BSM, but also for Higgs precision because vector boson fusion processes logarithmically grow with energy.

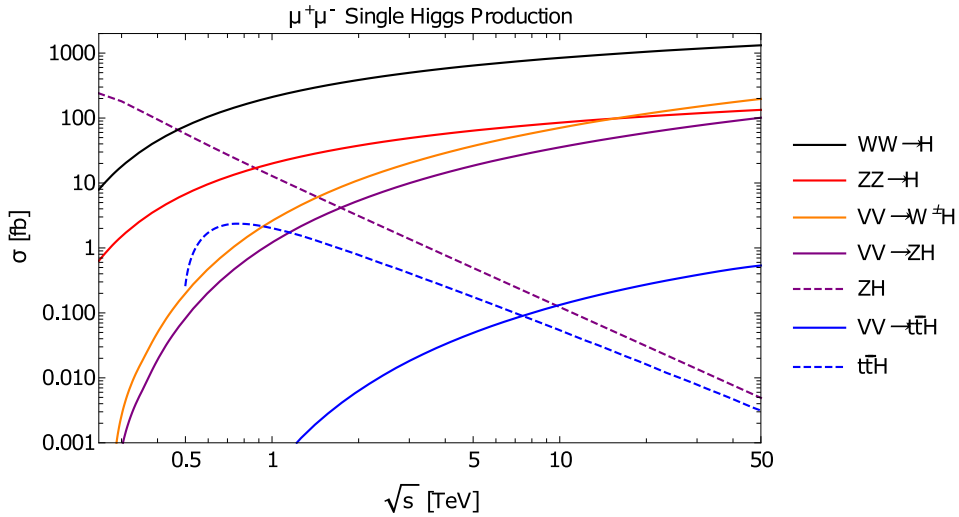

- Compared to electron colliders, muon colliders can achieve higher energy while requiring smaller sizes since muons are heavier. (The power carried by the synchrotron radiation $P \propto \gamma^4$.)

	Length	Energy
FCC-ee	91.2 km	91 GeV – 365 GeV
CLIC	11 km – 50 km	380 GeV – 3 TeV
ILC	30 km – 50 km	250 GeV – 1 TeV
IMCC	4.5 km – 14 km	3 TeV – 14 TeV
μTRISTAN	3 km – 6 km	1 TeV – 3 TeV

- Compared to pp colliders, muon colliders expect to have less background.

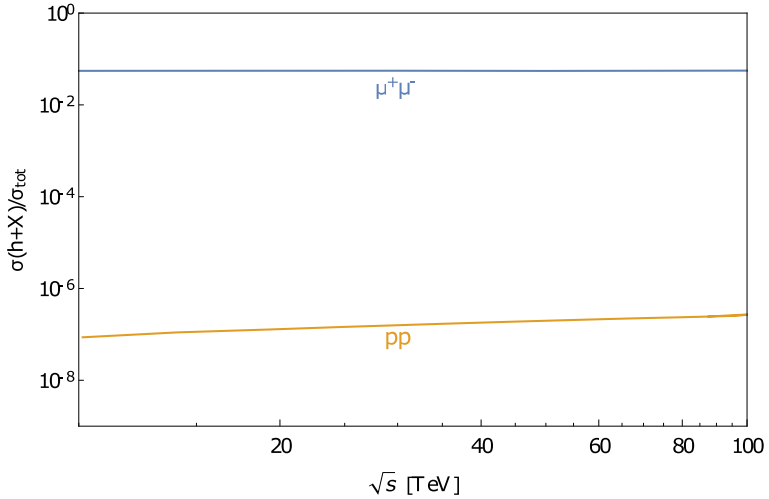

[H. A. Ali, "The Muon Smasher's Guide", Rept. Prog. Phys. 85, 084201 (2022)]

- In pp colliders, theoretical predictions of cross sections always include PDF uncertainty.

$\sqrt{s}$ (TeV)	Production cross section (in pb) for $m_H = 125\,\text{GeV}$					
	ggF	VBF	WH	ZH	$t\bar{t}H$	total
1.96	$0.95^{+17\%}_{-17\%}$	$0.065^{+8\%}_{-7\%}$	$0.13^{+8\%}_{-8\%}$	$0.079^{+8\%}_{-8\%}$	$0.004^{+10\%}_{-10\%}$	$1.23^{+15\%}_{-15\%}$
7	$16.9^{+5.5\%}_{-7.6\%}$	$1.24^{+2.2\%}_{-2.2\%}$	$0.58^{+2.2\%}_{-2.3\%}$	$0.34^{+3.1\%}_{-3.0\%}$	$0.09^{+5.6\%}_{-10.2\%}$	$19.1^{+5\%}_{-7\%}$
8	$21.4^{+5.4\%}_{-7.6\%}$	$1.60^{+2.1\%}_{-2.1\%}$	$0.70^{+2.1\%}_{-2.2\%}$	$0.42^{+3.4\%}_{-2.9\%}$	$0.13^{+5.9\%}_{-10.1\%}$	$24.2^{+5\%}_{-7\%}$
13	$48.6^{+5.6\%}_{-7.4\%}$	$3.78^{+2.1\%}_{-2.1\%}$	$1.37^{+2.0\%}_{-2.0\%}$	$0.88^{+4.1\%}_{-3.5\%}$	$0.50^{+6.8\%}_{-9.9\%}$	$55.1^{+5\%}_{-7\%}$
13.6	$52.2^{+5.6\%}_{-7.4\%}$	$4.1^{+2.1\%}_{-1.5\%}$	$1.46^{+1.8\%}_{-1.9\%}$	$0.95^{+4.0\%}_{-3.6\%}$	$0.57^{+6.9\%}_{-9.9\%}$	$59.2^{+5\%}_{-7\%}$
14	$54.7^{+5.6\%}_{-7.4\%}$	$4.28^{+2.1\%}_{-2.1\%}$	$1.51^{+1.8\%}_{-1.9\%}$	$0.99^{+4.1\%}_{-3.7\%}$	$0.61^{+6.9\%}_{-9.8\%}$	$62.1^{+5\%}_{-7\%}$

[PDG Review 2023]

μTRISTAN

- We proposed a new muon collider experiment called **μTRISTAN**, where we use **the ultra slow muon** technology as a cooling method instead of the ionization cooling.
- Ultra slow muons are obtained by ionizing muoniums ($e^-\mu^+$ bound state), whose kinetic energy is estimated as $25\,\mathrm{meV}$, thermal energy at room temperature.
- The ultra slow muon technology has already been demonstrated. It is estimated to achieve **a normalized transverse emittance of $\sim 1\,\mu\mathrm{m}$**.
- Recently, ultra slow muons are successfully accelerated to 90 keV at J-PARC.
- A limitation of this technology is that it can only be applied to **μ^+ and not μ^-**.
- However, we have demonstrated that the $e^-\mu^+$ and $\mu^+\mu^+$ collider can produce a sufficient number of Higgs particles, allowing us to measure the couplings with greater precision than the current constraints.

Outline

1. Collider design
2. Higgs boson production in the $e^-\mu^+$ collider
3. Higgs boson production in the $\mu^+\mu^+$ collider
4. New physics searches

Outline

1. **Collider design**
2. **Higgs boson production in the $e^-\mu^+$ collider**
3. **Higgs boson production in the $\mu^+\mu^+$ collider**
4. **New physics searches**

Luminosity

- To achieve high luminosity, the beam size should be small in both the longitudinal and transverse directions.
- The luminosity is given as

$$\mathcal{L} = f \frac{N_1 N_2}{4\pi \sigma_x \sigma_y}$$

$N_{1,2}$:# of particles in a bunch of the beam 1,2

$\sigma_{x,y}$: The beam size at the collision point

f: The frequency of the collisions

$$\sigma_x = \sqrt{\beta_x^* \varepsilon_x}$$

β_x^*: The beta function at the collision point,

ε_x: **The transverse emittance (referring to the area occupied by the beam in a position-momentum phase space)**,

The beta function is given as $\beta(z) = \beta^* + z^2/\beta^*$.

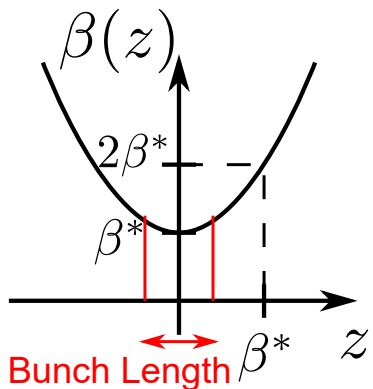

- The emittance reduces under acceleration, which is another benefit of higher energy. The normalized emittance $\gamma\beta\varepsilon_x$ is invariant.
- **A better cooling gives a smaller emittance and a smaller bunch length.**

Ultra slow muons

The method was demonstrated at KEK BOOM in 1995, and at ISIS RIKEN-RAL in 2008, and is further developing at J-PARC.
The muons are slowed to nearly a complete stop, then accelerated to produce a beam that is well-aligned.

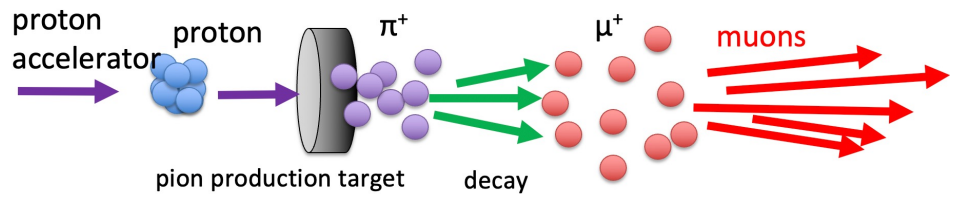

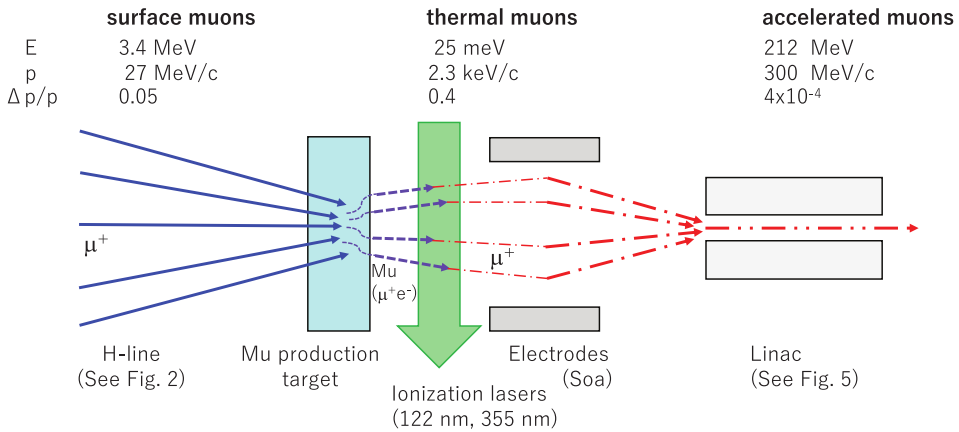

- Protons are accelerated to 3 GeV and guided to the pion production target.
- **Surface muons**: low energy muons ($\sim 3.4\,\mathrm{MeV}$) from pions stopped near the target.
- The surface muon beam is transferred to a silica aerogel target to produce **muoniums**.
- The muoniums are ionized by laser excitation. $\Rightarrow$ **Ultra Slow Muons**
- The normalized emittance $\gamma\beta\varepsilon_{x,y}$ is estimated as $\sim 1\,\mu\mathrm{m}$.
- The expected number of ultra slow muons is estimated as $\sim 10^{-7}$ per proton.

How to enhance the number of ultra slow muons

- We assume a J-PARC like proton driver:
  Energy: $3\,\mathrm{GeV}$, Intensity: 4.1×10^{13} per bunch, Number of bunches: 2, Repetition rate: $50\,\mathrm{Hz}$, Beam power: $2\,\mathrm{MW}$
- Two bunches of the proton beam repeatedly collides with the pion production target 40 times, and muons from two bunches of proton are gathered and merged to make a single bunch. $\Rightarrow$ **40 bunches of muons are obtained per 2 bunches of protons**.
- **Layers of pion stopping and muonium formation targets** are placed.
- We shoot **lasers between the layers** to ionize the muoniums.
- We assume 1.1×10^{-3} **muons** are produced per single proton collision. According to an ongoing simulation by Yasuhiro Sakaki and Mitsuhiro Yoshida, we can obtain this number.
- The ultra slow muons are corrected and transferred to the second muonium-formation target, and ionized by laser again. Here the production efficiency of 50% is assumed, and then the number of muons per proton becomes $\sim 5.5 \times 10^{-4}$.
  $\Rightarrow$ $\mathbf{4.5 \times 10^{10}}$ muons per bunch.

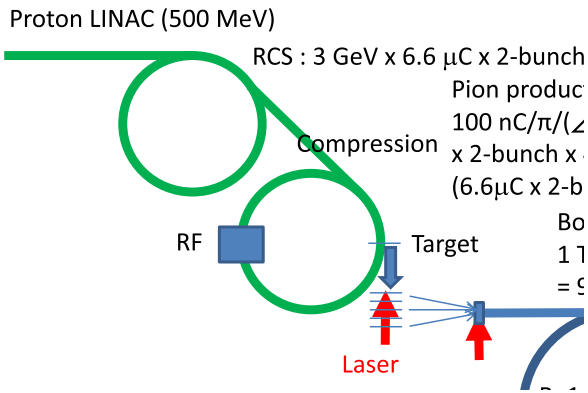

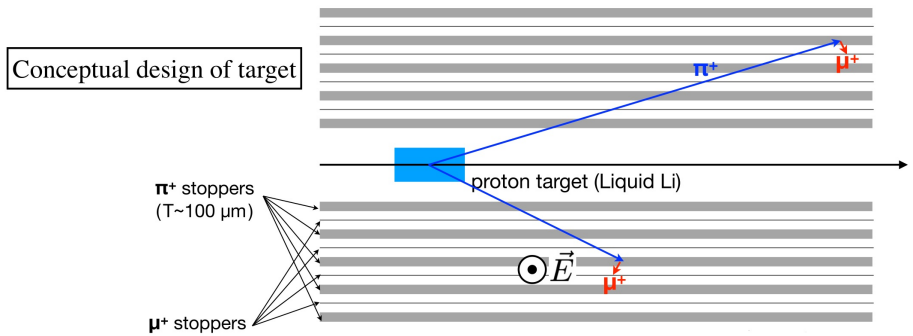

Booster ring

- In our design, muons are accelerated to **1 TeV** and electrons are accelerated to **30 GeV**. Those values are determined from the current technology of the magnet and the size of the main ring, 3km circumference.
- The booster ring consists of two LINAC parts of length 3km and two arc sections of diameter 1km.
- In each of the LINAC parts, the μ^+ beam is accelerated by $\mathbf{30\,GeV}$.

$$1\,\mathrm{TeV} \simeq 30\,\mathrm{GeV} \times 2 \text{ parts} \times 16 \text{ turns}$$

- The acceleration takes $\mathbf{700\,\mu s}$, during which the intensity reduces to $\mathbf{2.3 \times 10^{10}}$ muons per bunch.
- In accordance with the repetition rate of $50\,\mathrm{Hz}$ we keep the muon beam in the main ring for $\mathbf{20\,ms}$, which is equal to the muon lifetime. Due to the decay of the muons during this time, the time-averaged number of muons is $\mathbf{1.4 \times 10^{10}}$ muons per bunch.

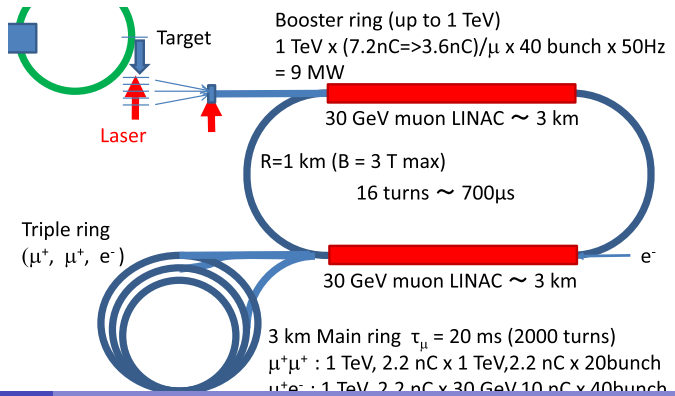

Luminosity estimation

- The luminosity of the $e^-\mu^+$ collider is estimated from

$$f_{e\mu} = \#\text{ of collision per second} = \frac{\text{Speed of light}(3\times10^5\text{ km/s})}{\text{Circumference}(3\text{ km})} \times 40\text{ bunches} = 4\text{ MHz},$$

$$f_{\mu\mu} = 2\text{ MHz}$$

$$N_\mu = \text{The averaged \# of muons per bunch} = 2.3\text{ nC} = 1.4\times10^{10},$$

$$N_e = \#\text{ of electrons per bunch} = 10\text{ nC} = 6.2\times10^{10},$$

$$\sigma_x = \sqrt{\frac{4\ \mu\text{m}\times 30\text{ mm}}{1\text{ TeV}/100\text{ MeV}}} \sim 3\ \mu\text{m}, \quad \sigma_y = \sqrt{\frac{4\ \mu\text{m}\times 7\text{ mm}}{1\text{ TeV}/100\text{ MeV}}} \sim 2\ \mu\text{m}$$

$$\mathcal{L}_{e^-\mu^+} = f_{e\mu}\frac{N_\mu N_e}{4\pi\sigma_x\sigma_y} = 4.6\times10^{33}\text{cm}^{-2}\text{s}^{-1}$$

$$\mathcal{L}_{\mu^+\mu^+} = f_{\mu\mu}\frac{N_\mu N_\mu}{4\pi\sigma_x\sigma_y} = 5.7\times10^{32}\text{cm}^{-2}\text{s}^{-1}$$

- Integrated luminosities are

$$\mathcal{L}^{\text{int}}_{e^-\mu^+} \sim 1\text{ ab}^{-1} \text{ for } \sim\text{10 years of running}$$

$$\mathcal{L}^{\text{int}}_{\mu^+\mu^+} \sim 0.1\text{ ab}^{-1} \text{ for } \sim\text{10 years of running}$$

Comparison to the IMCC design

- We use more conservative values for several parameters that could be used commonly in the both of $\mu^+\mu^+$ and $\mu^+\mu^-$ colliders than the IMCC design.
- The normalized emittance and the bunch length of the ultra cold muon beam are expected to achieve the requirement by IMCC.
- In the IMCC design, the bunch charge is taken to be large.
  (HL-LHC: 1.15×10^{11}, FCC-ee:1.5×10^{11} – 2.3×10^{11}.)
- If we use the same parameters as the IMCC design, except for the normalized emittance and the beta function, and assume that the beta function can match the bunch length, the luminosity would be
  1000-40000 $\times 10^{34}\mathrm{cm}^{-2}\mathrm{s}^{-1}$ at 10 TeV.

	IMCC	μTRISTAN ($e^-\mu^+$)	μTRISTAN ($\mu^+\mu^+$)
Normalized emittance (μm)	25	1 – 4	1 – 4
Bunch length (at 2 TeV) (mm)	7.5	0.1 – 1	0.1 – 1
Beta function at IP (mm)	5, 1.5, 1.1	(30, 7)	(30, 7)
Center-of-mass energy (TeV)	3, 10, 14	0.35	2
Circumference (km)	4.5, 10, 14	3	3
(Initial) bunch intensity (10^{10})	220, 180, 180	e^-:6.2, μ^+:2.3	2.3
Number of bunches	1	40	20
Repetition rate (Hz)	5	50	50
# of muons per second ($10^{13}/s$)	2	4	4
Luminosity (10^{34} cm^{-2} s^{-1})	2,20,40	0.4	0.06

[C. Accettura et al., "Towards a Muon Collider", Eur. Phys. J. C 83, 864 (2023)]

Polarization

- The **polarization** of the beams is important to enhance the Higgs production via fusion processes.
- The electron beam polarization is set to be $\boldsymbol{P_e = -0.7}$, which has been studied for an upgrade of the superKEKB.
- The muon beam polarization is assumed to be $\boldsymbol{P_\mu = 0.8}$.
  The polarization of μ^+ can be maintained in the muonium formation by a longitudinal magnetic field.
- Even if the longitudinal magnetic field is not used, there remains $P_\mu = 0.25$.
  - All muons from the pion decay are **right-handed**.
  - The half of the muonium state is $|{+}{+}\rangle$ whose spin is preserved, while $|{+}{-}\rangle$ states undergo spin oscillation, and thus under the single process of the muonium formation and laser ionization, **the polarization becomes half**.
  - After the two muonium formation processes, the polarization becomes $P_\mu = 0.25$.
- Even if $P_\mu = 0.25$, the Higgs production cross section is only reduced by 30% in the $e^-\mu^+$ collider.

Outline

1. Collider design
2. **Higgs boson production in the $e^-\mu^+$ collider**
3. Higgs boson production in the $\mu^+\mu^+$ collider
4. New physics searches

Higgs production in $e^-\mu^+$ collider: W-fusion

In the $e^-\mu^+$ collider, **the W boson fusion** is the dominant channel of Higgs production.

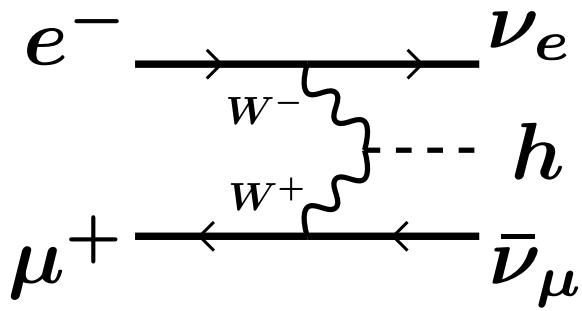

- The beam energies are **30 GeV** and **1 TeV** for e^- and μ^+.
  $\Rightarrow$ $\sqrt{s} = 346$ **GeV**.
- The cross section is $\sigma_{\mathrm{WBF}} = 91$ **fb.** $\Rightarrow$ **# of Higgs** $\sim 90,000$ **at 1** $\mathbf{ab^{-1}}$.
  (For comparison, the cross section of $\mu^-\mu^+ \to \nu_\mu\bar{\nu}_\mu H$ at $\sqrt{s} = 2\,\mathrm{TeV}$ is $387\,\mathrm{fb}$.)
- From this, the statistical error of the kappa parameters are estimated as

$$\Delta(\kappa_W + \kappa_b - \kappa_H) = \frac{1}{2}\frac{1}{\sqrt{N(\mathrm{WBF}) \times \mathrm{Br}(H \to b\bar{b}) \times \text{efficiency}}}$$
$$= 0.0031 \times \left(\frac{\text{Integrated luminosity}}{1.0\ \mathrm{ab}^{-1}}\right)^{-1/2} \times \left(\frac{\text{Efficiency}}{0.5}\right)^{-1/2}$$

Detector simulation

- The detector simulation using MadGraph + PYTHIA + Delphes is in progress.
- We have used the HL-LHC card.

	Signal	Background	$S/\sqrt{S+B}$
No cut	9.0933e+04	1.0249e+07	2.8279e+01
Exact 2 b jets	1.2025e+04	5.3215e+04	4.7079e+01
No muon and electron	1.1997e+04	3.7747e+04	5.3789e+01
$\mathrm{MET} > 15\,\mathrm{GeV}$	1.1156e+04	9.4088e+03	7.7792e+01
$M_{b\bar{b}} > 80\,\mathrm{GeV}$	8.5768e+03	2.4507e+03	8.1674e+01

- This signal to noise ratio corresponds to $\Delta(\kappa_W + \kappa_b - \kappa_H) = 0.006$

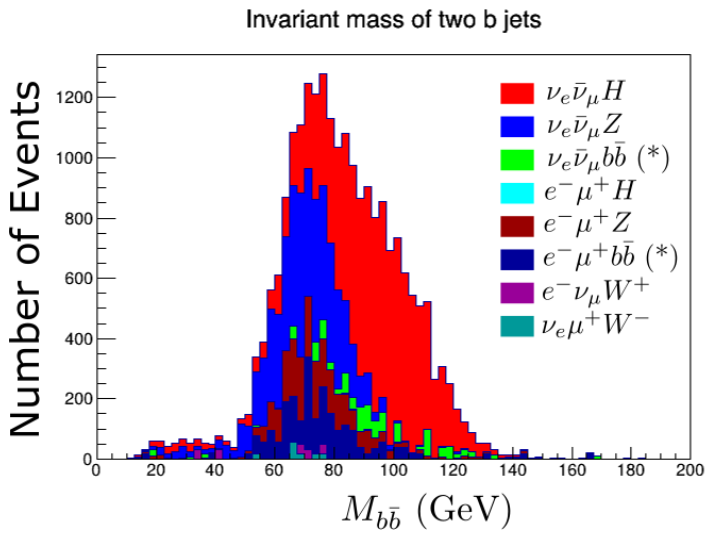

Z boson fusion and recoil mass

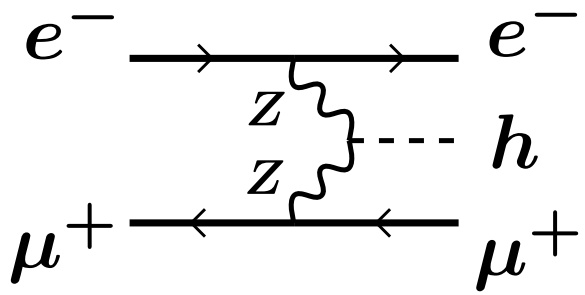

- At $\sqrt{s} = 346$ GeV, $\sigma_{\mathrm{ZBF}} \sim 4$ fb. $\Rightarrow$ # of Higgs = 4,000 at 1 ab^{-1}.
- For the ZZ-fusion process, by using the momentums of e^- and μ^+ in the final state, we can reconstruct the Higgs mass. $\Rightarrow$ **Total width measurement**.
- For $\mu^-\mu^+$ colliders with larger beam energies $\sim 10\,\mathrm{TeV}$, the recoil mass analysis is difficult since the energy resolution of the forward muons is not enough.
- In the case of $e^-\mu^+$ collider with smaller energy, muons with $|\eta| < 4$ can be used to reconstruct the Higgs mass.

Z boson fusion and recoil mass

A detector simulation is ongoing.

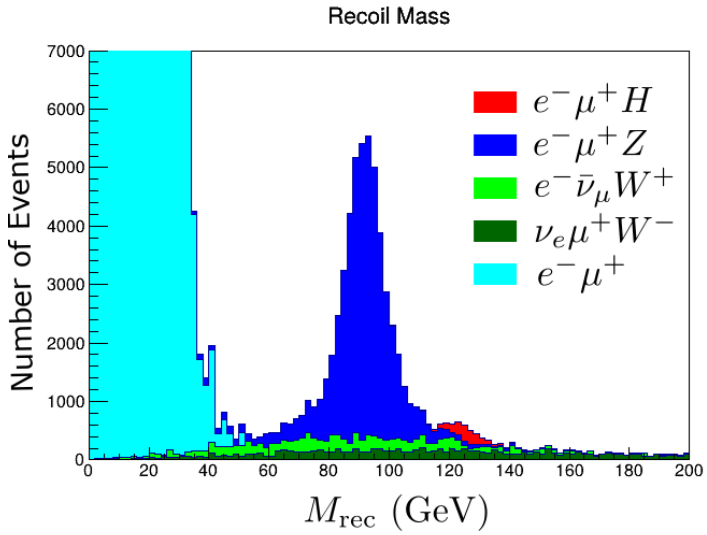

	Signal	Background	$S/\sqrt{S+B}$
No cut ($\lvert\eta_l\rvert < 4$)	3.1967e+03	2.2661e+08	2.1235e-01
At least 1 muon	2.6582e+03	1.9242e+08	1.9163e-01
At least 1 electron	2.0212e+03	1.5192e+08	1.6398e-01
Shield ($\eta < 2$)	3.1967e+03	2.2661e+08	2.1235e-01
$115\,\mathrm{GeV} < M_{\mathrm{rec}} < 135\,\mathrm{GeV}$	1.7489e+03	1.4078e+04	1.3902e+01
$\eta_{\mathrm{elec}} > 1.5$	1.6677e+03	1.0420e+04	1.5168e+01
$E_\mu > 250\,\mathrm{GeV}$	1.4840e+03	3.5678e+03	**2.0879e+01**

Outline

1. Collider design
2. Higgs boson production in the $e^-\mu^+$ collider
3. **Higgs boson production in the $\mu^+\mu^+$ collider**
4. New physics searches

Higgs production in $\mu^+\mu^+$: W-fusion via photon

- Even for $\mu^+\mu^+$, we can realize WW-fusion by introducing a photon propagator.
- Despite the additional coupling, the contribution from this graph has the comparable value to the usual WW-fusion.

  At $\sqrt{s} = 2\,\mathrm{TeV}$, $\sigma_{\mathrm{WWFvP}} \simeq 60\,\mathrm{fb}$ for $\mathrm{pol} = 0.8$, while $\sigma_{\mathrm{WWF}} \simeq 400\,\mathrm{fb}$ for $\mathrm{pol} = 0$.
- This is because the cross section of the process grows with $(\log s)^3$, while the WW-fusion grows with $\log s$ at high energy.
- The calculation of this graph is tricky because it divergences at $p_T(\mu^+) = 0$ in $m_\mu \to 0$ limit.

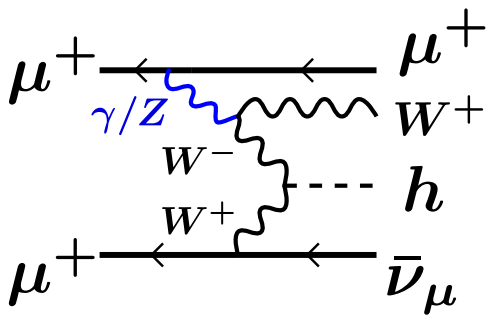

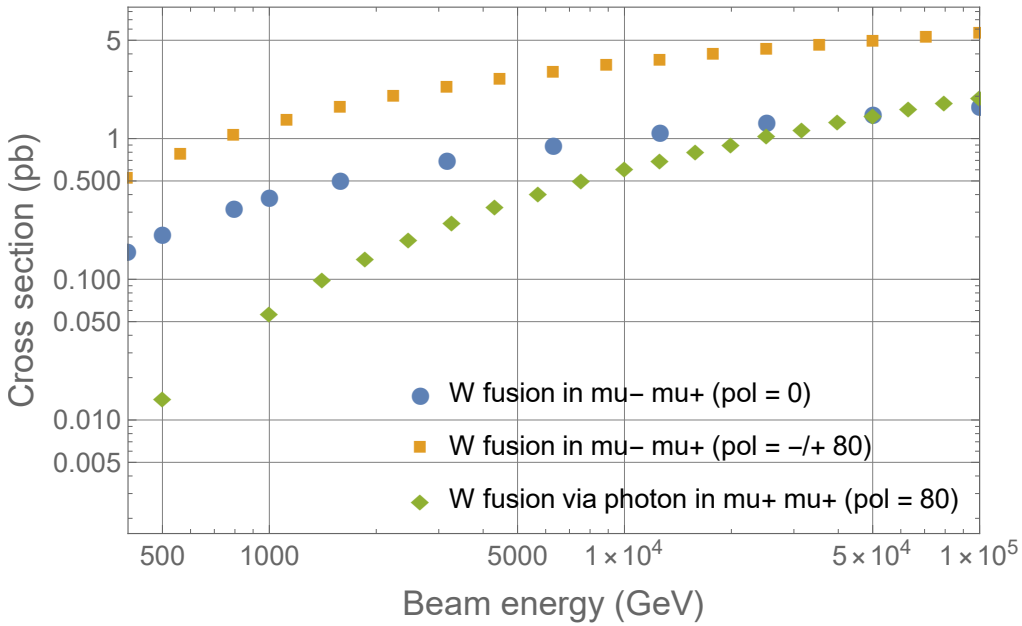

Log counting

- Using **the Effective Vector Boson Approximation**, where the vector bosons are treated as partons, we can estimate the number of logarithmic factors at high energy.
- For example, the usual WW fusion cross section is

$$\sigma_{\ell^-\ell^+\to\nu_\ell\bar{\nu}_\ell h}(s) = \int_{m_h^2/s}^1 d\xi f_{W_L^-/\ell^-}(\xi)\,\sigma_{W_L^-\ell^+\to h\bar{\nu}_\ell}(\xi s) \sim \log s,$$

$$f_{W_L^-/\ell^-}(\xi) = \frac{g^4}{4\pi^2}\frac{1-\xi}{\xi} \sim \frac{1}{\xi}, \quad \sigma_{W_L^-\ell^+\to h\bar{\nu}_\ell}(\xi s) \sim \text{const.}$$

- For **the WW fusion via photon**,

$$\sigma_{\mu^+\mu^+\to\mu^+W^+\bar{\nu}_\mu h}(s) = \int d\xi d\xi' f_{\gamma/\mu}(\xi') f_{W_L^+/\mu}(\xi)\,\sigma_{W_L^+\gamma\to hW^+}(\xi'\xi s) \sim \log^3 s,$$

$$\sigma_{W_L^+\gamma\to hW^+}(\xi'\xi s) \sim \text{const.}, \quad f_{\gamma/\mu}(\xi) = \frac{\alpha}{2\pi}\frac{1+(1-\xi)^2}{\xi}\log\frac{\mu_f^2}{m_\mu^2},\ \mu_f^2 = \xi'\xi s.$$

Effective Photon Approximation

- Due to the pole of the propagator of photon, MadGraph fails to estimate low p_T region of μ^+. $\Rightarrow$ The low p_T region should be estimated by the **EPA (Effective Photon Approximation**.

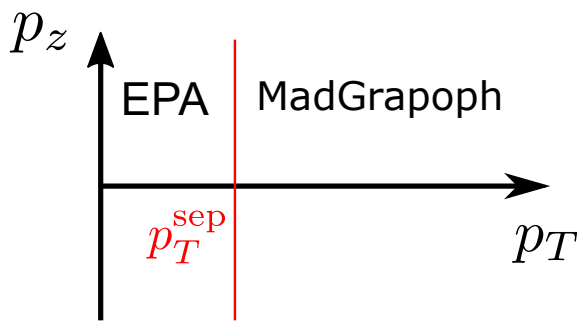

Let us take the integration region as $0 < p_T < p_{\rm T}^{\rm (cut)}$.

- By neglecting higher order terms of q^2 and $p_{\rm T}^{\rm (cut)}$, the cross section can be written as ($\sigma_{\rm part}$: The cross section of the graph where the photon is treated as an external line.)

$$\sigma = \int_{s_{\rm min}/s}^{1} dy\, f(y)\sigma_{\rm part}(ys),$$

$$f(y) = \frac{\alpha_{\rm em}}{2\pi}\left[-2\,\frac{1-y}{y}\,\frac{\left(p_{\rm T}^{\rm (cut)}\right)^2}{\left(p_{\rm T}^{\rm (cut)}\right)^2 + m_\ell^2\, y^2} + \frac{1+(1-y)^2}{y}\,\log\frac{\left(p_{\rm T}^{\rm (cut)}\right)^2 + m_\ell^2\, y^2}{m_\ell^2\, y^2}\right]$$

EPA + MadGraph

- We separated the phase space into two region at $p_T = p_T^{\rm sep}$, and used MadGraph in $p_T > p_T^{\rm sep}$ and used EPA approximation in $p_T < p_T^{\rm sep}$.

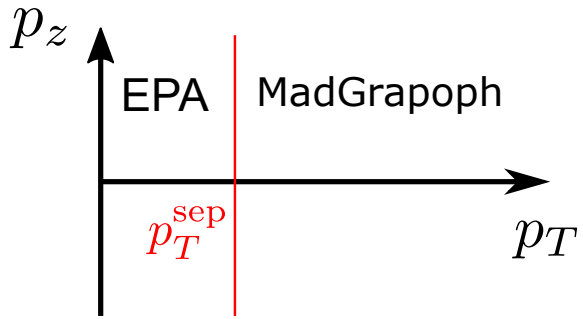

- We confirmed that the result does not depend on the choice of $p_T^{\rm sep}$ in the region $0.5\,{\rm GeV} < p_T^{\rm sep} < 20\,{\rm GeV}$.

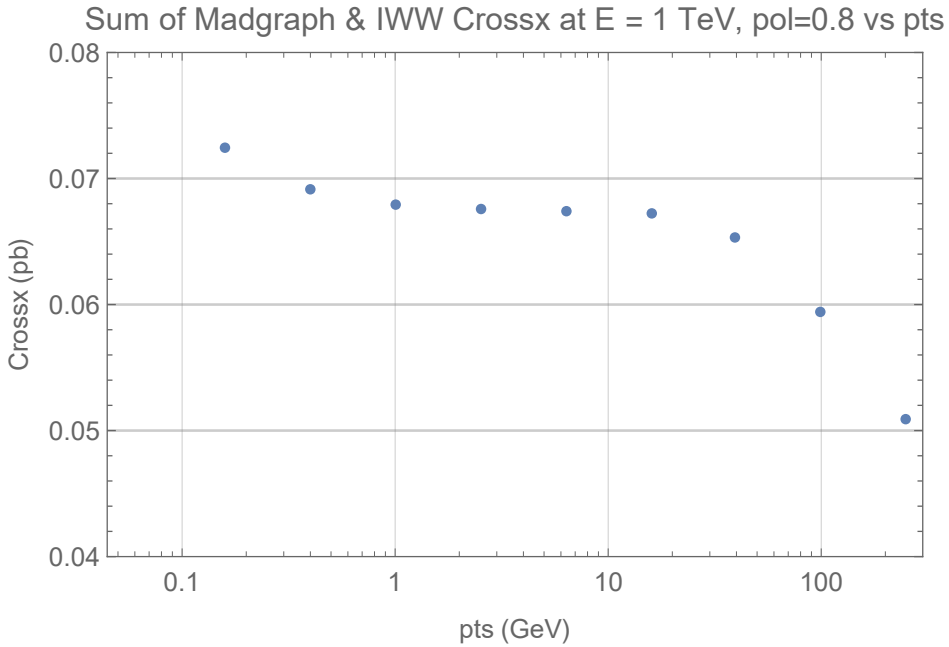

Outline

1. Collider design
2. Higgs boson production in the $e^-\mu^+$ collider
3. Higgs boson production in the $\mu^+\mu^+$ collider
4. **New physics searches**

Slepton production

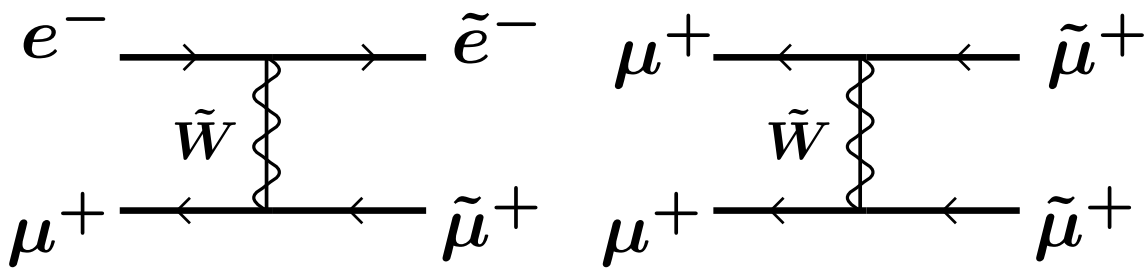

The region where the amount of charged **slepton pair production per year is larger than 100** at $e^-\mu^+$ and $\mu^+\mu^+$ colliders.

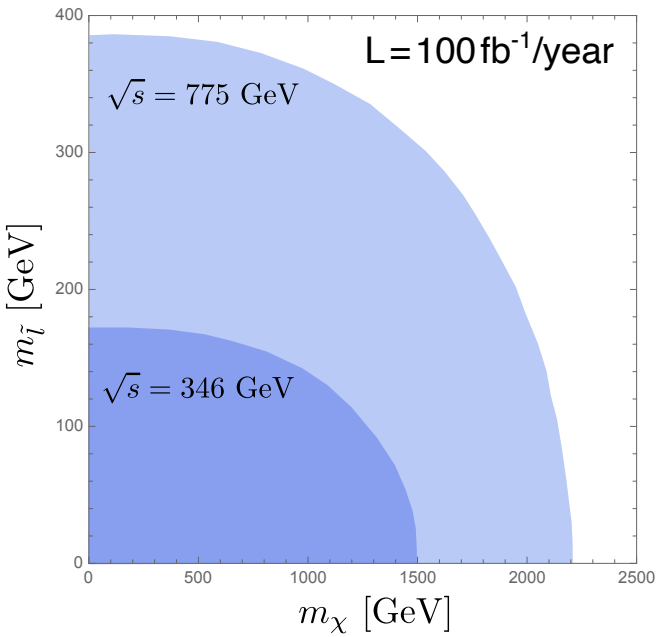

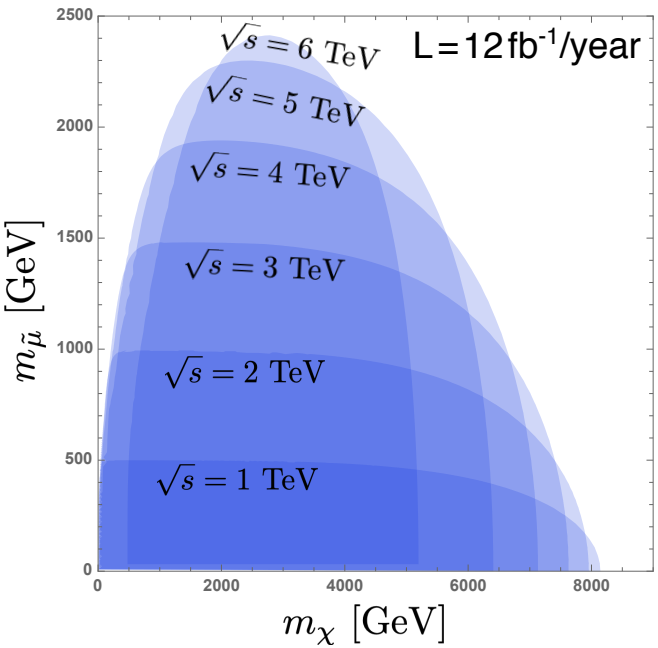

Constraints on dimension-6 SMEFT ops. from the elastic scattering

Precision measurement of the cross section of $e^-\mu^+ \to e^-\mu^+$ and $\mu^+\mu^+ \to \mu^+\mu^+$ can give a limit to the SMEFT ops.

$$S \supset \int \sum_J \frac{1}{\Lambda_J^2} Q_J.$$

The SM couplings modified by

$$\begin{cases} Q_{HWB} = H^\dagger H B_{\mu\nu} B^{\mu\nu},\ Q_{HD} = (H^\dagger D_\mu H)^* (H^\dagger D_\mu H), \\ Q_{Hl}^{(1)} = (H^\dagger i\overleftrightarrow{D}_\mu H)(\bar{L}\gamma^\mu L),\ Q_{Hl}^{(3)} = (H^\dagger i\overleftrightarrow{D}^I_\mu H)(\bar{L}\tau^I\gamma^\mu L),\ Q_{He} = (H^\dagger i\overleftrightarrow{D}_\mu H)(\bar{R}\gamma^\mu R) \end{cases}$$

Four fermi interactions:

$$Q_{\substack{ll \\ prst}} = (\bar{l}_p\gamma_\mu l_r)(\bar{l}_s\gamma^\mu l_t), \quad Q_{\substack{le \\ prst}} = (\bar{l}_p\gamma_\mu l_r)(\bar{e}_s\gamma^\mu e_t), \quad Q_{\substack{ee \\ prst}} = (\bar{e}_p\gamma_\mu e_r)(\bar{e}_s\gamma^\mu e_t)$$

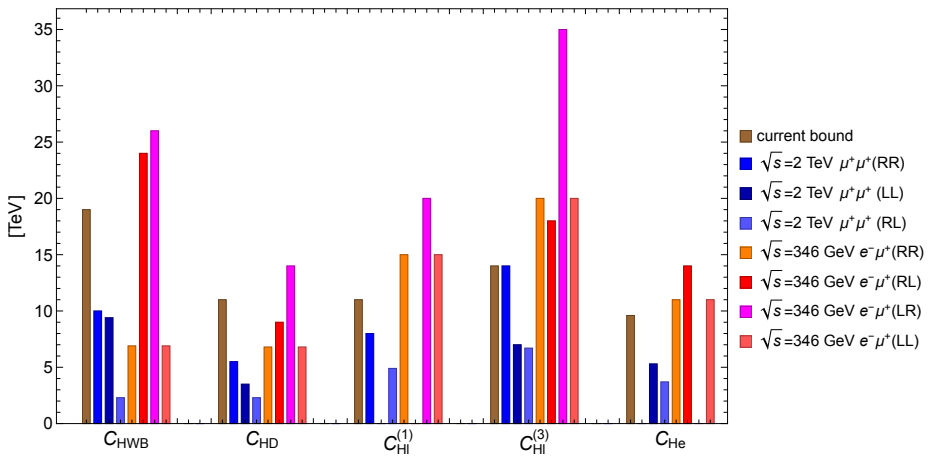

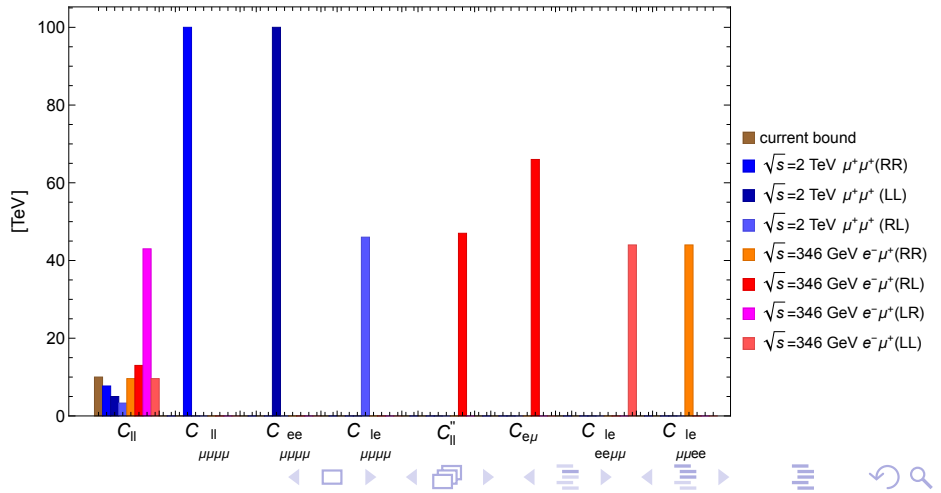

Summary

- For μ^+, an efficient cooling method exists: Ultra Slow Muons.
- The $e^-\mu^+$ and $\mu^+\mu^+$ can give sub-percent level precision measurements of Higgs couplings.

Other topics:

- Polarization: Is $P_\mu = 0.8$ possible without affecting emittance?
- Neutrino-induced radiation
- Detector study for beam induced background
- Neutrino usage

  [Ryuichiro Kitano, Joe Sato, Sho Sugama, "T-violation of future neutrino factory", arXiv:2407.05807]

  (Next Talk)
- More new physics searches

  [Kåre Fridell, Ryuichiro Kitano, Ryoto Takai, "Lepton flavor physics at $\mu^+\mu^+$ colliders", JHEP 06 (2023) 086]

  [Hajime Fukuda, Takeo Moroi, Atsuya Niki, and Shang-Fu Wei, "Search for WIMPS at $\mu^+\mu^+$ collider", JHEP 02 (2024) 214]

Back Up

Physics beyond the Standard Model

The Standard Model cannot explain

- Dark matter
- Neutrino mass
- Baryon asymmetry
- (Muon g-2 anomaly)

The higher energy collider is beneficial to uncover new physics.
The properties of Higgs should be investigated more to answer the questions:

- Is Higgs elementary or composite?
- Why is the Higgs mass unnaturally small?
- What is the origin of the electroweak symmetry breaking?

π^+ production position

(production = increse - decrease)

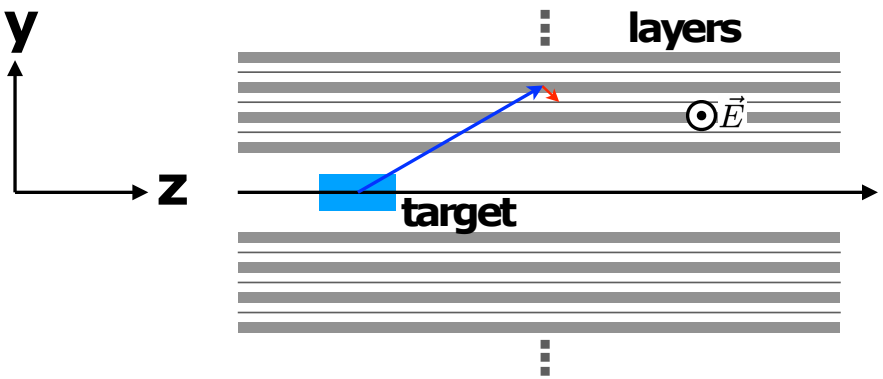

85% is produced on target and **15% on layer** (in this setup)

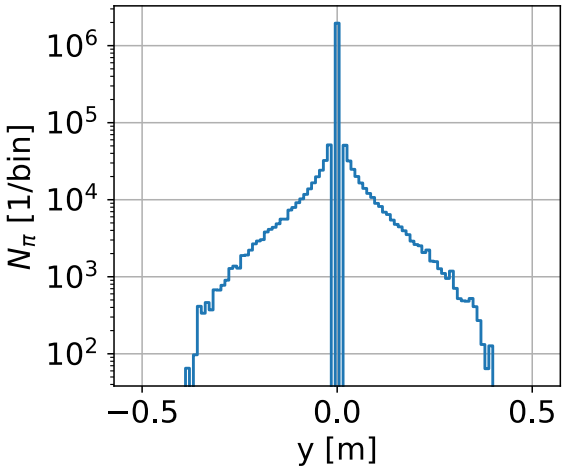

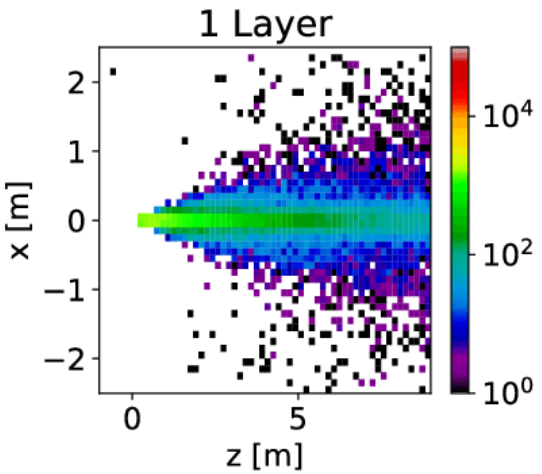

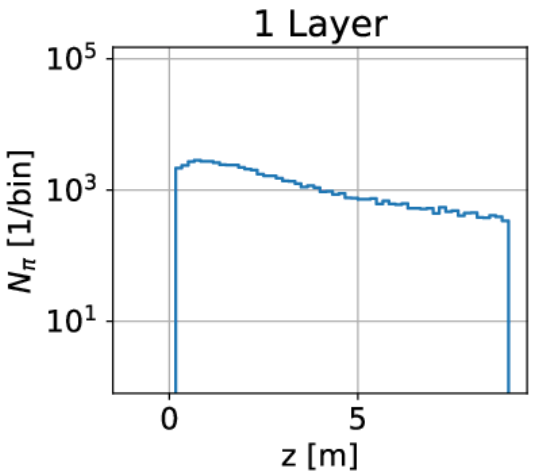

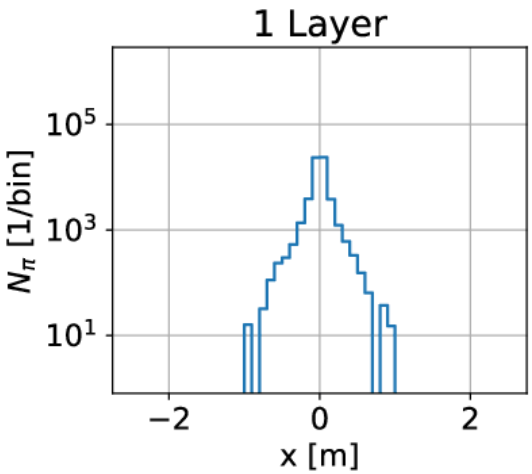

[Animation] https://rcwww.kek.jp/research/shield/sakaki/_/2023/zx_pi.gif

Taken from Yasuhiro Sakai's slide

μ^+ "stopping" position by ionization

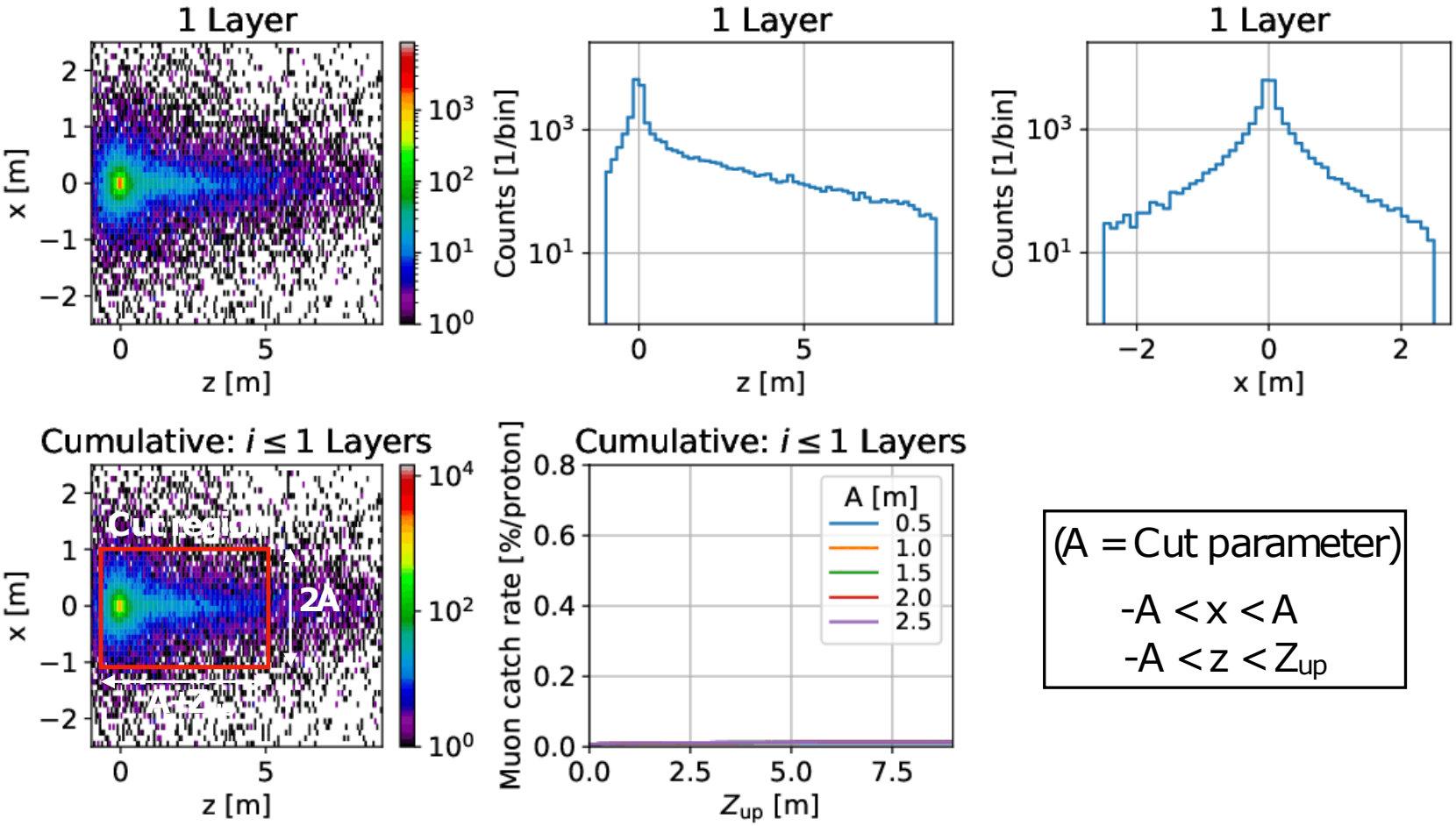

(A = Cut parameter)

$-A < x < A$

$-A < z < Z_{up}$

Making the system smaller does not signif cantly reduce the capture rate

[Animation] https://rcwww.kek.jp/research/shield/sakaki/_/2023/zx_mu.gif

Taken from Yasuhiro Sakai's slide